Humic Acid Coated Fe₃O₄ Nanoparticle for Phenol Sorption

Soerja Koesnarpadi[*], Sri Juari Santosa, Dwi Siswanta, and Bambang Rusdiarso

Department of Chemistry, Faculty of Mathematics and Natural Sciences, Universitas Gadjah Mada,
Sekip Utara, PO BOX BLS 21, Yogyakarta 55281, Indonesia

ABSTRACT

The coating Fe_3O_4 using humic acid (HA) to form HA-coated Fe_3O_4 (Fe_3O_4/HA) was conducted and applied for phenol sorption. Fe_3O_4/HA was prepared using co-precipitation method in an alkaline condition using ammonium hydroxide and the addition of HA with mass ratios of Fe_3O_4 and HA = 20:1, 10:1, 10:2, 10:3. The HA from peat soil in Sambutan village, East Kalimantan, Indonesia and was extracted in NaOH 0.1 M solution. The FT-IR characterization indicated that the coating of HA on the surface of Fe_3O_4 was successfully synthesized by forming a bond between the carboxylate group of HA and iron of Fe_3O_4. The coating of HA on the surface of Fe_3O_4 did not change the crystal structure of Fe_3O_4, but had lower peak intensities than Fe_3O_4 if added with HA with mass ratios 20:1, 10:1, 10:2, 10:3. The saturation magnetization of Fe_3O_4 decreased with the increased content of HA. SEM image indicated the magnetic particle size was almost homogenous by 10-18 nm. Iron and HA in Fe_3O_4/HA materials synthesized using different mass ratios were stable in pH range of 3.0-11.0 and 1.0–11.0, respectively. The phenol sorption on Fe_3O_4 was optimum at pH 5.0 and on Fe_3O_4/HA with mass ratios of 20:1, 10:1, 10:2, 10:3 were optimum at pH 5.0-6.0. The kinetics model for phenol adsorption on Fe_3O_4 and Fe_3O_4/HA with mass ratios of 20:1, 10:1, 10:2, 10:3 could be described using pseudo second-order equation and was in accordance with the Langmuir isotherm model with maximum adsorption capacity of 0.45 mmol/g for Fe_3O_4 and 0.55, 0.56, 0.58, 0.56 mmol/g respectively for Fe_3O_4/HA with mass ratios of 20:1, 10:1, 10:2, 10:3. The adsorption capacity increased with the increased content of HA, but the adsorption energy decreased except Fe_3O_4/HA with a mass ratio of 10:3. Generally, the performance of Fe_3O_4/HA materials was much higher than of bare Fe_3O_4.

Keywords: coating; humic acid; Fe_3O_4; adsorption; phenol

ABSTRAK

Telah dilakukan penyalutan Fe_3O_4 menggunakan Asam humat (AH) membentuk adsorben Fe_3O_4/AH dan diaplikasikan untuk adsorpsi fenol. Penyalutan Fe_3O_4/AH dilakukan dengan metode kopresipitasi dalam kondisi basa menggunakan ammonium hidroksida dan adanya penambahan AH dengan perbandingan massa Fe_3O_4 dan AH = 20:1, 10:1, 10:2 dan 10:3. AH diperoleh dari tanah gambut daerah Sambutan, Kalimantan Timur, Indonesia dan dilakukan ekstraksi pada larutan basa NaOH 0,1 N. Karakterisasi spektra FT-IR terlihat bahwa penyalutan AH pada permukaan Fe_3O_4 telah berhasil disintesis dengan adanya pembentukan ikatan antara gugus karboksilat pada AH dengan Fe pada Fe_3O_4. Penyalutan AH pada permukaan Fe_3O_4 tidak mengalami perubahan struktur kristal namun memiliki intensitas puncak lebih rendah daripada Fe_3O_4 jika ditambah AH perbandingan 20:1, 10:1, 10:2 dan 10:3. Harga Kemagnetan Fe_3O_4 turun dengan penambahan AH. Foto SEM menunjukkan bahwa ukuran partikel magnetik relatif homogen sekitar 10-18 nm. Kestabilan ion Fe pada Fe_3O_4/AH adalah pH 3,0-11,0 sedangkan AH pada Fe_3O_4/AH dengan perbedaan perbandingan massa adalah pH 1,0–11,0. Adsorpsi fenol pada Fe_3O_4 optimum pada pH 5 sedangkan pada Fe_3O_4/AH optimum pada pH 5,0-6,0. Model kinetika adsorpsi fenol pada Fe_3O_4 dan Fe_3O_4/AH dengan perbandingan massa 20:1, 10:1, 10:2, 10:3 dapat dijelaskan dengan persamaan model kinetika pseudo orde-dua dan sesuai dengan persamaan isoterm Langmuir dengan kapasitas adsorpsi maksimum sebesar 0,45 mmol/g untuk Fe_3O_4 dan berturut-turut 0,55, 0,56, 0,58, 0,56 mmol/g untuk Fe_3O_4/AH pada perbandingan massa 20:1, 10:1, 10:2, 10:3. Kapasitas adsorpsi meningkat dengan meningkatnya jumlah AH tetapi energy adsorpsi semakin turun kecuali pada Fe_3O_4/AH dengan perbandingan massa 10:3. Secara umum, kinerja adsorben Fe_3O_4/AH lebih baik daripada Fe_3O_4 tanpa penyalutan AH.

Kata Kunci: penyalutan; asam humat; Fe_3O_4; adsorpsi; fenol

* Corresponding author.
Email address : soerja.koes@gmail.com

INTRODUCTION

Phenol is extremely toxic to the environment and this pollutant released from oil refineries, pulp and paper mills, pharmaceutical, and pesticides. Phenol is classified as a carcinogenic compound and at a certain level can have adverse effects on human health [1]. As a result, the European Union has included phenol in the list of priority pollutants. The European Community sets the maximum amount of phenol in wastewater by lower than 1 ppm [2]. Several methods have been proposed to separate phenol from wastewater such as membrane techniques [3], solvent extraction [4], biological treatments [5], heterogenous photocatalysis [6] and adsorption [7-8]. Adsorption is one of the methods that are efficient, low in cost and high in capacity [9].

Nowadays, magnetic nanomaterials derived from certain iron oxides (Fe_3O_4, γ-Fe_2O_3, α-Fe_2O_3) are increasingly popular used as nano sorbents not only in water-treatment technologies [10] but also in biomedical applications [11] or in analytical chemistry [12] due to their excellent sorption ability, good mechanical properties and facile separability with a simple magnetic process [13]. Fe_3O_4 nano particles attract pollutants significantly due to their advantages in recovering and recycling [14]. They are widely used in manufacturing magnetic recording devices, protective and sensitive coating, pigments, catalyst and applications in biomedical fields [13]. They have unique properties due to their response to the magnetic field, high saturation magnetization, non-toxic and high biocompatibility [15]. The magnetite nanoparticles are easily oxidized and agglomerated in aqueous solution. Therefore, stabilized magnetite is desirable [16].

Several researchers have focused on the modification of Fe_3O_4 which has specific surface combined with organic materials such as polyacrylic acid [17], chitosan [18], alginate [19] or humic acid [20] for pollutant removal. Humic acid (HA) is a natural organic macromolecule made of decomposed plant and animal materials in soil [21]. Chemically, it is a heterogeneous compound that has multiple functional groups containing carboxyl and hydroxyl groups as its predominant functional groups. The functional groups of HA have different ability to bind metal ion in forming a complex of metal-HA [22]. HA in Indonesia has functional groups of which oxygen content specifically distributed into COOH, phenolic OH and alcoholic OH. The oxygen containing functional groups is mostly in the form of carboxyl and phenolic OH. The composition of oxygen in the functional groups of HA is highly dependent on its origin [23]. The interaction of HA and Fe_3O_4 surface can effectively prevent the collision of particle adhesion during the heating process. The modification of humic acid on the surface of Fe_3O_4 can change its properties entirely or partially depending on its chemical properties and amount adsorbed. The binding of HA on Fe_3O_4 effects the adsorbing properties of Fe_3O_4 because HA bond produces a polyanionic organic coating on Fe_3O_4 and thus essentially changes the surface properties of Fe_3O_4. Recent research indicated HA has high affinity to Fe_3O_4 nanoparticles and enhances the stability of nanodispersion by preventing agglomeration [24-25].

Recently, several researchers have been conducted to examine the possibility of Fe_3O_4/HA to be used as an efficient material for removing heavy metal [20], serving as a catalyst for mineralization of sulfathiazole [26], removing rhodamine B [27] and adsorbing methylene blue [28]. The novelty of this research compared to previous studies is that the adsorbent of Fe_3O_4 nanoparticles was coated using HA extracted from peat soil from Sambutan village, East Kalimantan. The previous researchers used commercial HA taken from Acros Organics and Aldrich [20] or Humatex [28]. The materials of Fe_3O_4/HA were developed by differentiating mass ratios of Fe_3O_4 and HA = 20:1, 10:1, 10:2, 10:3 and then applied to phenol sorption in aqueous solution. The physical and chemical characterization was examined in Fe_3O_4 and HA-modified Fe_3O_4 (Fe_3O_4/HA) and the calculation of adsorption kinetics and isotherm of phenol sorption were evaluated on Fe_3O_4 and Fe_3O_4/HA.

EXPERIMENTAL SECTION

Materials

The reagents of analytical grade from Merck (Germany): $FeCl_3.6.H_2O$, $FeSO_4.7.H_2O$, NH_4OH 25%, C_6H_5OH, HCl, HF, NaOH, N_2. CH_3OH, 4-aminoanthypirine, $K_4(FeCN)_6$ and Humic acid (HA) from peat soil of Sambutan village, Samarinda, East Kalimantan was extracted by recommended procedure International Humic Substances Society (IHSS).

Procedure

Preparation and characterization of Fe_3O_4/HA

Fe_3O_4/HA was synthesized using co-precipitation method. 1.525 g $FeCl_3.6.H_2O$ and 1.05 g $FeSO_4.7H_2O$ were dissolved into 25 mL of distilled water and heated to 90 °C. NH_4OH 25% was added to the mixed solution until pH 11 and then 0.25 g of humic acid was added rapidly in 1 M of NaOH and 12.5 mL of distilled water. The mixture was stirred at 90 °C for 30 min and then cooled to room temperature. The black sediment resulted was separated from the solution and washed to neutral using distilled water. Fe_3O_4/HA was prepared

using different mass ratios of Fe_3O_4:HA=20:1, 10:1, 10:2 and 10:3.

The bare Fe_3O_4 magnetite nanoparticle was prepared using the same method as the synthesis of Fe_3O_4/HA without adding HA. The functional groups of Fe_3O_4/HA and Fe_3O_4 were characterized using a Shimadzu 8201 PC Fourier transform spectrometer (FT-IR). The crystal structure was analyzed using Shimadzu X-ray diffraction (XRD) and using CuKα radiation (λ = 1.5406 Å) operated at 40 kV and 30 mA. Vibrating sample magnetometer was used to measure magnetization curve. The surface morphology and particle size were examined using a JEOL SSM-6510 LA Scanning electron microscopy (SEM).

Stability of Fe ions and HA contained in Fe₃O₄/HA

Two series of solutions were prepared for stability test of Fe ions and HA contained in Fe_3O_4/HA. 10 mg of Fe_3O_4/HA was added to 10 mL of distilled water and the acidity was adjusted from pH 1.0 to 13.0 by using HCl or NaOH solution. The mixture was stirred for 60 min and after 24 h the supernatant was then separated from Fe_3O_4/HA. The HA dissolved in the supernatant was analyzed using UV-Spectrophotometer (1601 PC UV-Vis Double Beam) and then Fe ions in the supernatant were determined using Atomic Absorption Spectrophotometer (AAS-Analytik Jena).

Procedure for phenol sorption in Fe₃O₄/HA

Adsorption experiments were carried out at room temperature using a shaken batch process. 10 mg of Fe_3O_4/HA and 1 mL of H_2O_2 0.5 M were added into 10 mL solution of phenol 100 mg/L. A series of experiment was conducted to evaluate the effects of pH ranging from 3.0 to 8.0 with the addition of HCl or NaOH. The adsorption kinetics was measured at an initial phenol concentration of 100 mg/L with interaction time of 0, 30, 60, 90, 120, 180 and 240 min. The equation models of Lagergren's pseudo first-order, Ho's pseudo second-order and Santosa's first-order were used to analyze the adsorption kinetic model. The adsorption capacity was also measured using the batch method in the concentrations of phenol solution of 30, 50, 80, 100, 150 and 200 mg/L. After the supernatant was separated, the concentration of phenol was determined using the 4-aminoantypirine method and analyzed using Visible-Spectrophotometer (Optima SP-300 Spectrophotometer). The blank solution was also analyzed under the same condition as the sample solution. Based on the data obtained, the capacity and equilibrium constant (K) of adsorption were calculated based on the Langmuir isotherm adsorption model and the energy (E) of adsorption was calculated using the equation of $E = RT \ln K$.

RESULT AND DISCUSSION

In this research, HA and Fe_3O_4 were successfully coated using the coprecipitation method in alkaline condition at pH 11 and heated at 90 °C. The interaction of HA and Fe_3O_4 is able to be conducted under acidic or alkaline condition because Fe_3O_4 is amphoteric which can develop charge in the protonation and deprotonation reaction on the surface site of Fe-OH. At above the pH of pZc, the surface charge Fe_3O_4 is negative, the binding of HA in Fe_3O_4 in alkaline condition is dominated by the interaction between HA and Fe_3O_4, namely the reaction of ligand-exchange with the surface of hydroxyl [24,29].

The spectroscopic analysis of HA from Sambutan Village, East Kalimantan, on Fe_3O_4 and Fe_3O_4/HA with the mass ratios of 20:1, 10:1, 10:2, 10:3 is shown Fig. 1. FTIR spectra of HA indicated the presence of O-H stretching vibration at 3425 cm⁻¹, the wave number of 1720 and 1629 cm⁻¹ attributed to the C=O stretching vibration on COOH and COO⁻ asymmetric stretching vibrations and aromatic C=C stretching vibration respectively [19,28]. Both of Fe_3O_4 and Fe_3O_4/HA centered at 586 cm⁻¹ were attributed to the stretching vibration of Fe-O bond [25]. The successful coating of HA on Fe_3O_4 showed the C=O vibration at 1404 cm⁻¹, indicating that the carboxylate anion interacted with the Fe_3O_4 surface as the C=O vibration in free carboxylate acids and this suggests that carboxylate groups indeed play an important role in the bonding between HA and Fe_3O_4 [30]. It is believed the bonding between HA and Fe_3O_4 surface is mainly done through ligand exchange [20].
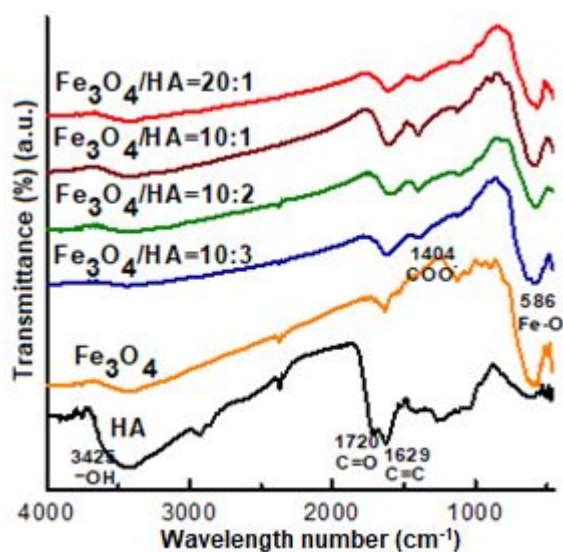
Fig 1. FTIR Spectra of HA extracted from peat soil of Sambutan village, East Kalimantan, Fe_3O_4 and Fe_3O_4/HA with mass ratios of 20:1, 10:1, 10:2 and 10:3
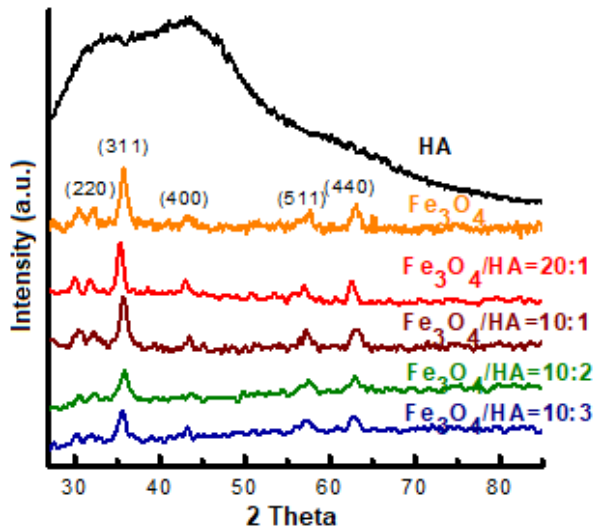
Fig 2. XRD pattern of HA from peat soil Sambutan village, Samarinda, East Kalimantan, Fe_3O_4 and Fe_3O_4/HA with mass ratios of 20:1, 10:1, 10:2 and 10:3
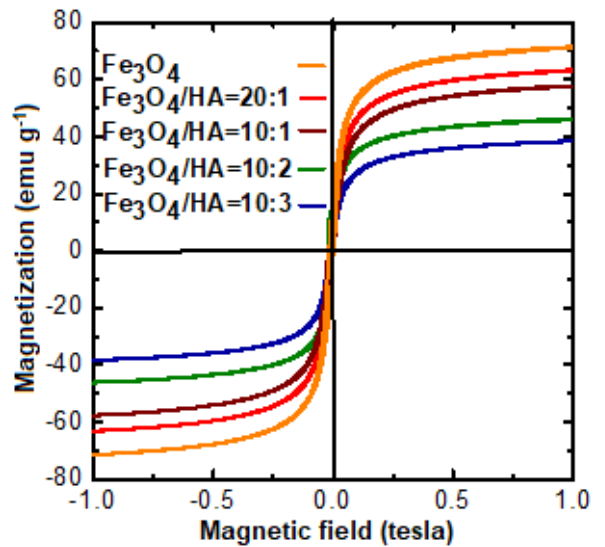
Fig 3. Magnetization curve of Fe_3O_4 and Fe_3O_4/HA with mass ratios of 20:1, 10:1, 10:2 and 10:3
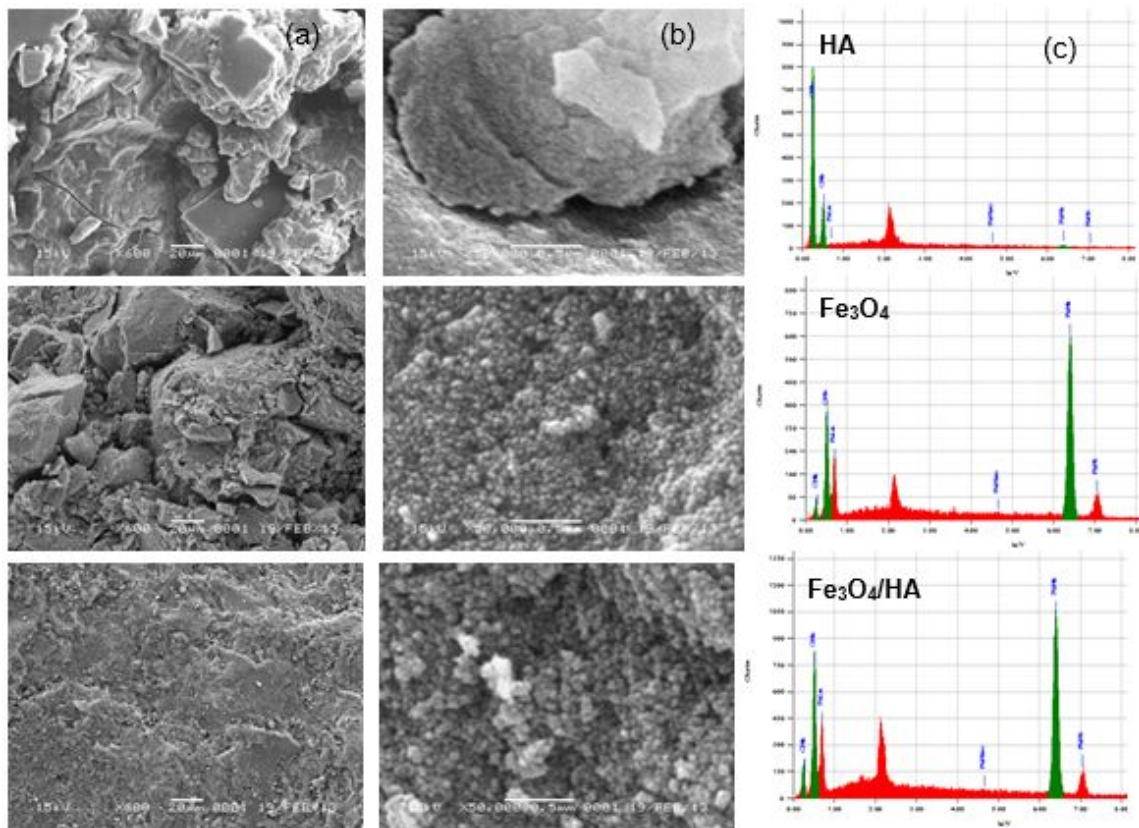
Fig 4. SEM image of HA, Fe_3O_4 and Fe_3O_4/HA with mass ratios of 20:1 (a) 600× magnification (b) 50.000× magnification and (c) analysis of Energy Dispersive X-Ray of C, O and Fe

The XRD measurement was used to identify the crystallinity of a product. The XRD patterns of HA was amorphous. Meanwhile, Fe_3O_4 and Fe_3O_4/HA with mass ratios of 20:1, 10:1, 10:2, 10:3 showed similar diffraction peaks at 2θ = 30.1°, 35.4°, 43.1°, 57.0°, 62.68° and 74.5° (Fig. 2). The XRD peaks are accordance with the peaks characteristic of inverse cubic spinel structure (JCPDS 65-3107) [15,31]. This result indicated that the
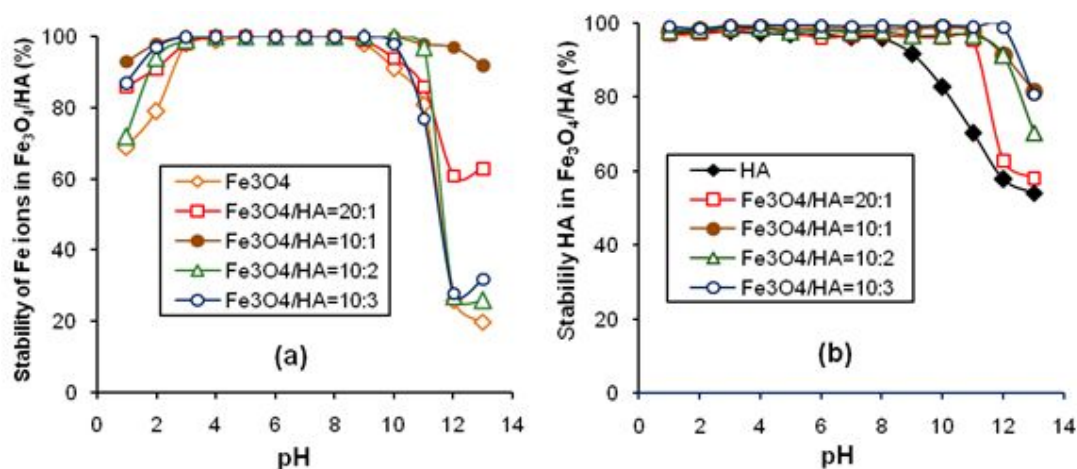
Fig 5. Effect of medium acidity on the stability of (a) Fe ions and (b) HA in Fe_3O_4/HA
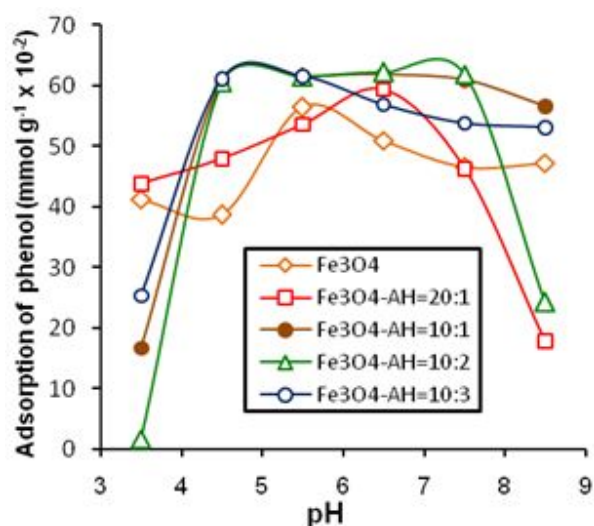
Fig 6. Effect of medium acidity on adsorption of phenol by Fe_3O_4, and Fe_3O_4/HA with mass ratios of 20:1, 10:1, 10:2 and 10:3

crystal structure of Fe_3O_4 did not undergo any changes after being modified using HA [15]. The coating of HA on the surface of Fe_3O_4 with mass ratios of 20:1, 10:1, 10:2, 10:3 decreased the XRD peak intensity of bare Fe_3O_4 and this indicated the crystallinity of Fe_3O_4/HA became lower.

The results of measurements of the specific saturation magnetization (Ms) of Fe_3O_4 was 71.25 emu/g and of Fe_3O_4/HA with mass ratios of 20:1, 10:1, 10:2, 10:3 were 63.31, 57.80, 46.20 and 38.39 emu/g respectively (Fig. 3). The presence of HA in Fe_3O_4 affected the magnetic properties of the adsorbent. The saturation magnetization decreased with the increased content of HA, but such decrease was still effective for the separation using magnetic field [32].

The SEM analysis of HA, Fe_3O_4 and Fe_3O_4/HA is shown in Fig. 4. SEM images of rigid colloid-shaped HA

and spherical-shaped Fe_3O_4 with nanosize which had a diameter of 10-18 nm were successfully made. However, whatever the shape of Fe_3O_4 is, it is still likely to agglomerate [26,33]. The coating of HA on Fe_3O_4 obtained larger particles size due to the combination of the coating agent layers on the surface of Fe_3O_4 [15]. The analysis of Energy Dispersive X-Ray indicated that HA was dominated by C (63%), O (34%) and a small amount of Fe (3%). Meanwhile, Fe_3O_4 was dominated by Fe (89%) and a small amount of C (3%) and O (8%). The coating of Fe_3O_4/HA decreased the composition of Fe to 83% but increased C and O to 6% and 11%. This indicated that the coating of HA on Fe_3O_4 was successful.

The coating of Fe_3O_4 using HA improved the stability of Fe ions and HA (Fig. 5). The bare Fe_3O_4 magnetite nanoparticles were stable at pH 3.0-9.0 and Fe_3O_4/HA was stable at pH 3.0-11.0. Under conditions of low pH, Fe^{2+} ion is released from Fe_3O_4 to form $\gamma\text{-}Fe_2O_3$ which has lower magnetism properties [34] and under condition of very high pH, the deprotonation of -COOH and -OH functional groups of HA in Fe_3O_4/HA makes H^+ ions from HA not able to stabilize Fe^{2+} ions [25]. On the other hand, without coating, HA is gradually dissolved from pH 9.0 to 13 because, under basic conditions, HA will easily dissolve. After coating HA on Fe_3O_4, Fe_3O_4/HA was relatively more stable at pH 1.0-11.

In this research, the analysis of phenol was determined using 4-aminoantipyrine method and analyzed using Visible-Spectrophotometer because this method was capable of measuring phenolic materials at the 5 µg/L level and applicable to the analysis of drinking waters and industrial wastes [35]. The effects of pH on the adsorption of phenol by Fe_3O_4, and Fe_3O_4/HA with mass ratios of 20:1, 10:1, 10:2, 10:3 are shown in Fig. 6. The adsorption of phenol on Fe_3O_4 and Fe_3O_4/HA were significantly affected by pH where

the adsorption of phenol on Fe_3O_4 was optimum at pH 5.0 and on Fe_3O_4/HA with mass ratios of 20:1, 10:1, 10:2, 10:3 were optimum at pH 5.0-6.0. This indicates that a change in pH of the solutions results in different surface charge of Fe_3O_4/HA. Under pH 5-6 solutions (pH < pH_{PZC}), the surface of Fe_3O_4/HA had positive charge due to the protonation of carboxylate functional groups of HA and had strong interaction with phenol molecule (< pKa 9.89). If the pH condition is very low, the protonation of functional group of HA in Fe_3O_4/HA is very strong that a repulsion occurs between functional groups of HA in Fe_3O_4/HA so that the adsorption of phenol in Fe_3O_4/HA declines. If the pH condition is very high, the surface of Fe_3O_4/HA has negative charge. The adsorption of phenol decreases due to ionization of phenol and repulsion of negative charge in Fe_3O_4/HA [24,36].

During the adsorption kinetics of phenol on Fe_3O_4 and Fe_3O_4/HA, the adsorption occurred very rapidly within 120 min and slowed down until the adsorbed phenol reached the equilibrium value as shown in Fig. 7. Lagergren's pseudo first-order, Ho's pseudo second-order and Santosa's first-order models were used to analyze the adsorption kinetics. The Lagergren's

equation for pseudo first-order kinetics can be written as the following Equation (1) [37]

$$\ln(q_e - q_t) = \ln q_e - k_1 t \qquad (1)$$

where q_e (amount of phenol adsorbed, mmol/g at equilibrium) and q_t (amount of phenol adsorbed, mmol/g
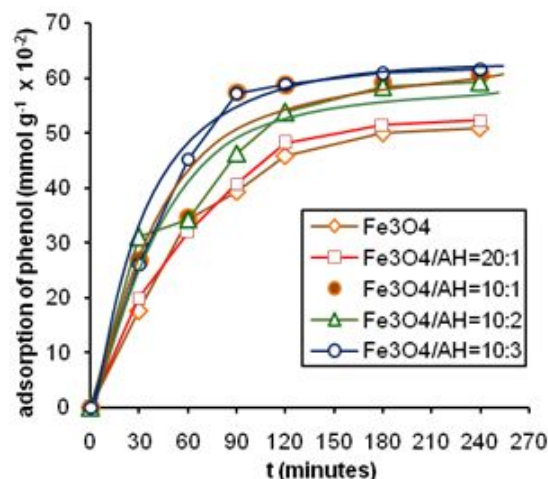
Fig 7. The influence of interaction time on adsorption of phenol onto Fe_3O_4 and Fe_3O_4/HA with mass ratios of 20:1, 10:1, 10:2 and 10:3
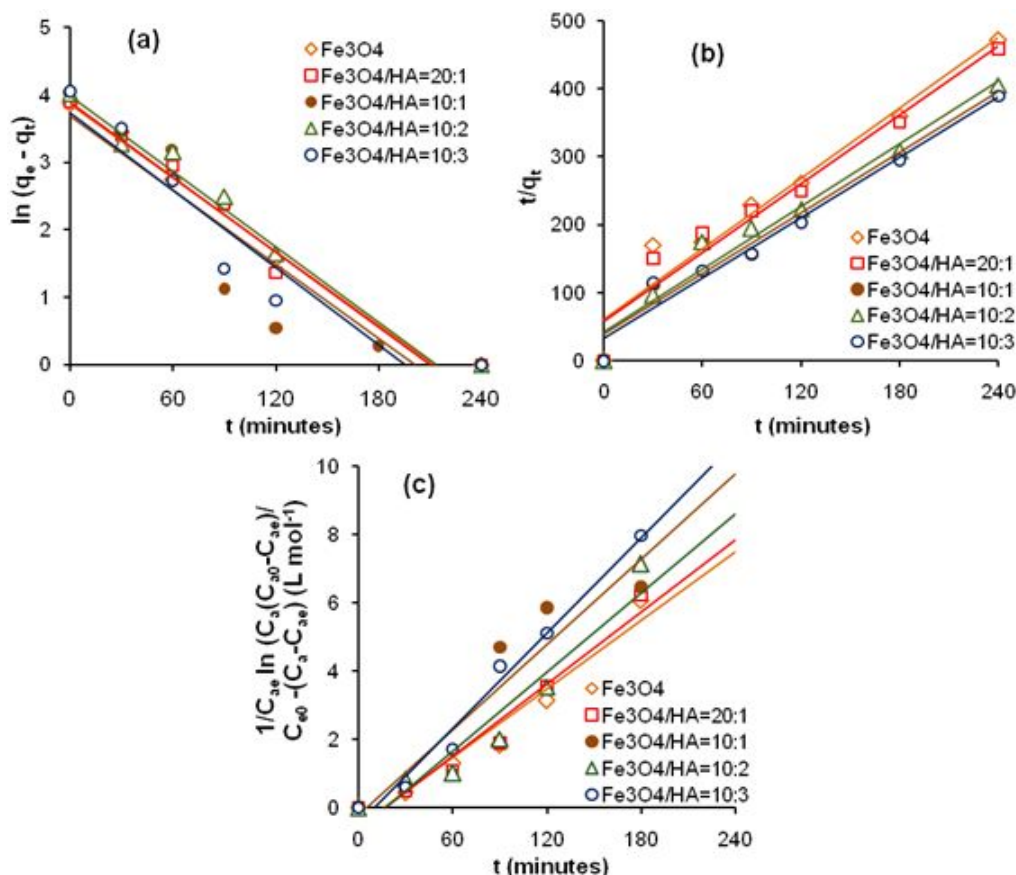
Fig 8. Plot of kinetics model for adsorption of phenol on Fe_3O_4 and Fe_3O_4/HA with mass ratios of 20:1, 10:1, 10:2 and 10:3 (a) pseudo first-order, (b) pseudo second-order and (c) first order

Table 1. Kinetic parameters of the pseudo first-order, pseudo second-order and first-order model for adsorption of phenol on Fe_3O_4 and Fe_3O_4/HA

Model	Parameters	Fe_3O_4	Fe_3O_4/HA = 20:1	Fe_3O_4/HA = 10:1	Fe_3O_4/HA = 10:2	Fe_3O_4/HA = 10:3
Lagergren's pseudo first-order	R^2	0.944	0.939	0.836	0.938	0.888
	q_e (mmol.g^{-1})	47.14	47.61	47.61	53.89	41.51
	k_1 (min^{-1})	0.018	0.017	0.017	0.018	0.019
Ho's pseudo second-order	R^2	0.944	0.951	0.952	0.964	0.972
	q_e (mmol.g^{-1})	0.580	0.593	0.674	0.649	0.675
	k_2 (g.mmol^{-1}.min^{-1})	0.049	0.049	0.055	0.056	0.068
Santosa's first-order	R^2	0.952	0.954	0.879	0.926	0.981
	k_2 (g.mmol^{-1}.min^{-1})	0.034	0.035	0.042	0.039	0.047
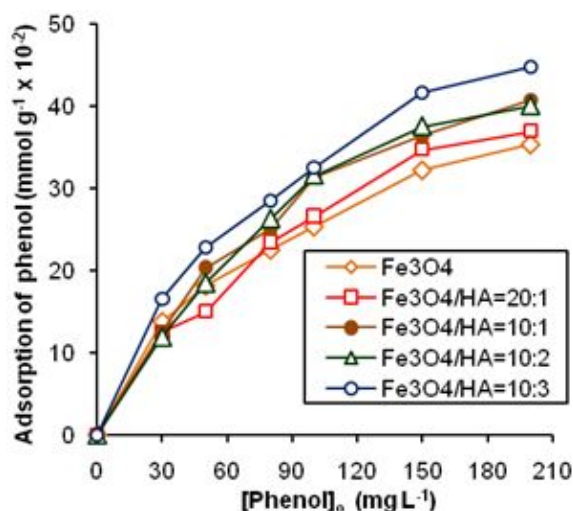
Fig 9. The influence of initial concentration on adsorption of phenol on Fe_3O_4 and Fe_3O_4/HA with mass ratios of 20:1, 10:1, 10:2 and 10:3

at time t) and k_1 (the pseudo first-order rate constant, min^{-1}). The Lagergren's first-order rate constant (k_1) and theoretical equilibrium adsorption capacity (q_e) were calculated from the intercept and slope of the plot ln (q_e-q_t) versus t.

The Ho's pseudo-second-order equation was used to describe the kinetics of phenol sorption, as in Equation (2), where q_e and q_t are similar to the previously mentioned, k_2 is pseudo second-order rate constant. (g/mmol.min). The plots of t/qt versus t is as follows [38]

$$\frac{t}{q_t} = \frac{1}{q_e}t + \frac{1}{k_2.q_e^2} \qquad (2)$$

The Santosa's first order model was represented in Equation (3), where C_{a0} is the initial concentrations of phenol (mmol/g), C_a and C_{ae} are the remaining concentrations of phenol in solution after the adsorption at t and equilibrium (mmol/g), k_s is the Santosa's first

order rate constant, and t is the interaction time. The plots of $\frac{1}{C_{ae}} \ln\left(\frac{C_a(C_{a0}-C_{ae})}{C_{a0}(C_a-C_{ae})} \right)$ versus t is as follows [39]

$$\frac{1}{C_{ae}} \ln\left(\frac{C_a(C_{a0}-C_{ae})}{C_{a0}(C_a-C_{ae})} \right) = k_s.t \qquad (3)$$

A linear relationship with high correlation coefficients which could be applied to sorption kinetics model was the pseudo-second-order model as shown Fig. 8 and the calculation of kinetics parameters for phenol adsorption on Fe_3O_4 and Fe_3O_4/HA are shown in Table 1. From the relationship shown in Fig. 8, the value of k_2 obtained for the phenol adsorption on Fe_3O_4 was 0.049 g.mmol^{-1}.min^{-1} and on Fe_3O_4/HA with mass ratios of 20:1, 10:1, 10:2, 10:3 were 0.049, 0.055, 0.056 and 0.0.068 g.mmol^{-1}.min^{-1} respectively. The phenol sorption rate on Fe_3O_4/HA was higher than that on Fe_3O_4.

The adsorption capacity of Fe_3O_4 and Fe_3O_4/HA with mass ratios of 20:1, 10:1, 10:2, 10:3 to adsorb phenol in various of initial phenol concentration was determined as shown in Fig. 9. From the data obtained, the phenol adsorbed at equilibrium (m, mmol/g) and the equilibrium phenol concentration (C_e, mmol/L) were fitted to the linear form of Langmuir and Freundlich isotherm model, as in Equation (4) and (5) [40]

$$\frac{C_e}{m} = \frac{1}{K.b}t + \frac{C_e}{b} \qquad (4)$$

$$\ln m = \ln K_f + \frac{1}{n}\ln C_e \qquad (5)$$

where b is the adsorption capacity, K and K_f are Langmuir and Freundlich equilibrium constants respectively (L.mmol^{-1} and mmol.g^{-1}/(mmol.L^{-1})^n), n (deviation from adsorption linearity) in the Freundlich exponential coefficient. From the relationship given in Fig. 10, the adsorption capacity (b) could be obtained from the slope. The equilibrium constant (K) could be calculated based on the intercept and the value of b and
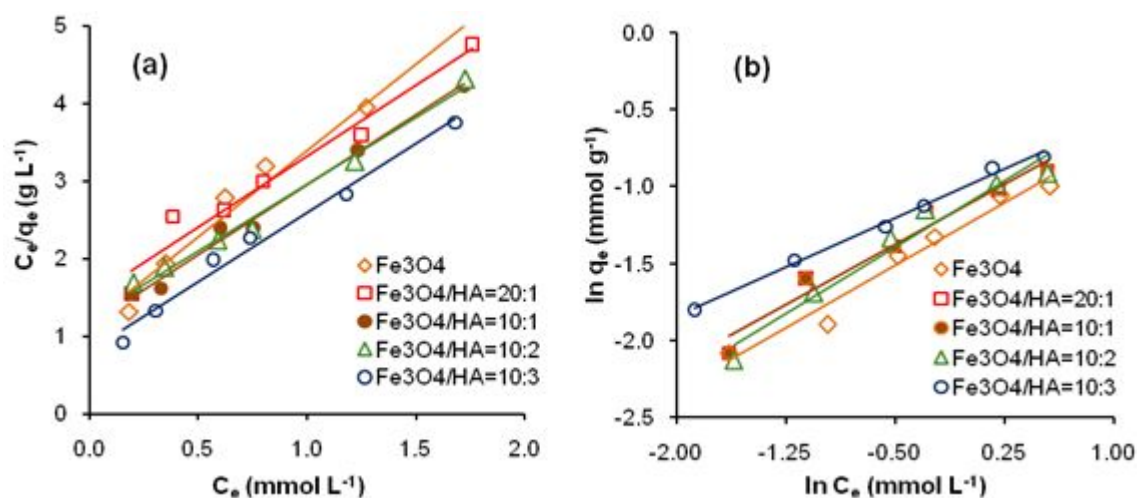
Fig 10. Plot of isotherm model for adsorption of phenol on Fe_3O_4 and Fe_3O_4/HA with mass ratios of 20:1, 10:1, 10:2 and 10:3 (a) Langmuir (b) Freundlich

Table 2. Adsorption isotherm parameters of phenol on Fe_3O_4 and Fe_3O_4/HA by Langmuir and Freundlich equations

Model	Parameters	Fe_3O_4	$Fe_3O_4/HA =$ 20:1	$Fe_3O_4/HA =$ 10:1	$Fe_3O_4/HA =$ 10:2	$Fe_3O_4/HA =$ 10:3
Langmuir	R^2	0,981	0.957	0.989	0.988	0.984
	b (mmol.g^{-1})	0.448	0.546	0.556	0.584	0.563
	K (L.mmol^{-1})	1909.2	1230.7	1560.8	1378.1	2182.7
	E (KJ.mol^{-1})	18.842	17.747	18.340	18.029	19.176
Freundlich	R^2	0.996	0.966	0.961	0.958	0.994
	K_f (mg.g^{-1})/(mg.L^{-1})^n	3.561	3.452	3.038	3.018	2.698
	n	2.375	1.852	1.912	1.741	2.362

the energy (E) could be calculated from the equation of $E = RT \ln K$. The results of b, K and E for the phenol adsorption on Fe_3O_4 and Fe_3O_4/HA with mass ratios of 20:1, 10:1, 10:2, 10:3 were summarized in Table 2.

The isotherm model of phenol sorption on Fe_3O_4 and Fe_3O_4/HA with mass ratios of 20:1, 10:1, 10:2, 10:3 was consistent with the Langmuir isotherm model with linier relationship R^2 0.981, 0.957, 0.989, 0.988, 0.984 and the maximum adsorption capacity was 0.45 mmol/g for Fe_3O_4 and 0.55, 0.56, 0.58, 0.56 mmol/g respectively for Fe_3O_4/HA with mass ratios of 20:1, 10:1, 10:2, 10:3. The adsorption capacity and linier relationship of phenol sorption on Fe_3O_4/HA were relatively higher than that determined for the phenol sorption on samla coal R^2 0.967; 13,28 mg/g, activated carbon R^2 0.987; 322.5 mg/g, rice husk R^2 0.959; 4.51 mg/g as found by Ahmaruzzaman and Sharma [41], representing smaller linear relationship. The Langmuir model assumes that the adsorption entirely involves active sites with homogenous surface of adsorbent; adsorption occurs through the same mechanism; adsorption occurs in monolayered form and adsorption does not occur between adsorbate molecules [36]. The presence of HA on Fe_3O_4 increased the adsorption capacity but decreased the adsorption energy, except on Fe_3O_4/HA

with a mass ratio of 10:3. This may be due to excessive HA in Fe_3O_4/HA which caused repulsion between functional groups of HA and then reduced the adsorption capacity of these adsorbents. The performance of four Fe_3O_4/HA materials to adsorb phenol was Fe_3O_4/HA = 10:2 > Fe_3O_4/HA=10:3 > Fe_3O_4/HA = 10:1 > Fe_3O_4/HA = 20:1. Generally, the performance of Fe_3O_4/HA materials were much higher than that of bare Fe_3O_4.

CONCLUSION

The coating of HA on Fe_3O_4 was successfully done by forming a bond between the carboxylate group of HA and Fe ions of Fe_3O_4. The coating HA on Fe_3O_4 did not affect the crystals structure of Fe_3O_4 and made the peaks intensities lower than Fe_3O_4 if added by HA with mass ratios 20:1, 10:1, 10:2, 10:3. The saturation magnetization of Fe_3O_4 decreased with the increased content of HA. SEM image indicated that Fe_3O_4 and Fe_3O_4/HA still had spherical shape in nanosize with almost homogenous particle size of 10-18 nm. This indicated that HA efficiently reduced the aggregation of Fe_3O_4. Iron and HA in both Fe_3O_4/HA materials synthesized using different mass ratios were stable

with a pH range of 3.0–11.0 and 1.0–11.0, respectively. The phenol sorption on Fe_3O_4 was optimum at pH 5.0 and on Fe_3O_4/HA with mass ratios of 20:1, 10:1, 10:2, 10:3 were optimum at pH 5.0-6.0. The kinetics model for phenol sorption on Fe_3O_4 and Fe_3O_4/HA could be described using pseudo second-order equation and consistent with the Langmuir isotherm model that the adsorption capacity increased in line with the increased content of HA, but decreased the adsorption energy. Generally, the performance of Fe_3O_4/HA materials were much higher than that of bare Fe_3O_4.

ACKNOWLEDGEMENT

REFERENCES

[1] Agency for Toxic Substances and Disease registry (ASTDR), 1998, *Toxicological Profile for Phenol*, NTIS report PB90-181249, Atlanta, Georgia, U.S, Department of Health and Human Service, Public health Service.

[2] Commission of the European, Urban Water Directive 91/271/EEC.

[3] Kujawski, W., Warszawski, A., Ratajczak, W., Porsbski, T., Capala, W., and Ostroeska, I., 2004, Removal of phenol from wastewater by different separation technique, *Desalination*, 163 (1-3), 287–296.

[4] Yang, C., Qian, Y., Zhang, L., and Feng, J., 2006, Solvent extraction process development and on site trial-plant for phenol removal from industrial coal-gasification waste water, *Chem. Eng. J.,* 117 (2), 179–185.

[5] Ramos, A.F., Gómez, A., Hontoria, E., and González-López, J., 2007, Biological nitrogen and phenol removal from saline industrial waste water by submerged fixed-film reactor, *J. Hazard. Mater.*, 142 (1-2), 175–183

[6] L'Amour, R.J.A., Azewedo, E.B., Liete, S.G.F., and Dezotti, M., 2008, Removal of phenol in high salinity media by a hybrid process (activated sludge + photocatalysis)*, Sep. Purif. Technol.*, 60 (2), 142–146

[7] Rosstaei, N., and Tezel, F.H., 2004, Removal of phenol from aqueous solution by adsorption, *J. Environ. Manage.*, 70 (2), 157-164

[8] Bahdod, A., El Asri, S., Saoiabi, A., Coradin, T., and Laghzizil, A., 2009, Adsorption of phenol from an aqueous solution by selected apatite adsorbents:

[9] Thomas, W.J., and Crittenden, B., 1998, "The development of adsorption technology" in *Adsorption Technology and Design*, Elsevier, 1–7.

[10] Ambashta, R.D., and Sillanpää, M., 2010, Water purification using magnetic assistance: A review, *J. Hazard. Mater.*, 180 (1-3), 38–49.

[11] Oh, J.K., and Park, J.M., 2011, Iron oxide-based superparamagnetic polymeric nanomaterials: Design, preparation, and biomedical application, *Prog. Polym. Sci.*, 36 (1), 168–189.

[12] Chen, L., Wang, T., and Tong, J., 2011, Application of derivatized magnetic materials to the separation and the preconcentration of pollutants in water samples, *Trends Anal. Chem.*, 30 (7), 1095–1108.

[13] Faraji, M., Yamini, Y., and Rezaee, M., 2010, Magnetic nanoparticles: Synthesis, stabilization, functionalization, characterization, and applications, *J. Iran. Chem. Soc.*, 7 (1), 1–37.

[14] Wang, N., Zhu, L., Wang, D., Wang, M, Lin, Z., Tang, H., 2010, Sono-assisted preparation of highly-efficient peroxidase-like Fe_3O_4 magnetic nanoparticles for catalytic removal of organic pollutants with H_2O_2, *Ultrason. Sonochem.*, 17 (3), 526–533.

[15] Petcharoen, K., and Sirivat, A., 2012, Synthesis and characterization of magnetite nanoparticles via the chemical co-precipitation method, *Mater. Sci. Eng., B*, 177 (5), 421–427.

[16] Maity, D., and Agrawal, C, 2007, Synthesis of iron oxide nanoparticles under oxidizing environment and their stabilization in aqueous and non-aqueous media, *J. Magn. Magn. Mater.*, 308 (1), 46–55.

[17] Mak, S.Y., and Chen, D.H., 2004, Fast adsorption of methylene blue on polyacrylic acid-bound iron oxide magnetic nanoparticles, *Dyes Pigm.*, 61 (1), 93–98.

[18] Chang, Y.C., Chang, S.W., and Chen, D.H., 2006, Magnetic chitosan nanoparticles: Studies on chitosan binding and adsorption of Co(II) ions, *React. Funct. Polym.*, 66 (3), 335–341.

[19] Ngomsik, A.F., Bee, A., Siaugue, J.M., Cabuil, F., and Cote, G., 2006, Nickel adsorption by magnetic alginate microcapsules containing an extractant, *Water Res.*, 40 (9), 1848–1856.

[20] Liu, J.F., Zhao, Z.S., and Jiang, G.B, (2008). Coating Fe3O4 magnetic nanoparticles with humic acid for high efficient removal of heavy metals in water, *Environ. Sci. Technol.*, 42, 6949–6954.

[21] Tan, K.H., 1993, *Principles of Soils Chemistry*, 3rd Ed., Marcel Dekker Inc, New York.

[22] Stevenson, F.J., 1994, *Humus Chemistry*, 2nd Ed., John Wiley and Sons, New York.

[23] Santosa, S.J., Tanaka, S., Siswanta, D., Kunarti, E.S, Sudiono, S., and Rahmanto, W.H., 2007, Indonesian peat soil derived humic acids, it's characterization, immobilization and performance as metal adsorbent, *Proceeding of International Conference on Chemical Sciences (ICCS),* Yogyakarta.

[24] Illés, E., and Tombácz, E., 2003, The role of variable surface charge and surface complexation in the adsorption of humic acid on magnetite, *Colloids Surf., A*, 203 (1-3), 99–109.

[25] Illés, E., and Tombácz, E., 2006, The effect of humic acid adsorption on pH-dependent surface charging and aggregation of magnetite nanoparticles*, J. Colloid Interface Sci.*, 295 (1), 115–123

[26] Niu, H., Zhang, D., Zhang, S., Zhang, X., Meng, Z., and Cai, Y., 2011, Humic acid coated Fe_3O_4 magnetic nanoparticles as highly efficient Fenton-like catalyst for complete mineralization of sulfathiazole, *J. Hazard Mater.*, 190 (1-3), 559–565.

[27] Peng, L., Qin, P., Lei, M., Zeng, Q., Song, H., Yang, J., Shao, J., Liao, B., and Gu, J., 2012, Modifying Fe_3O_4 nanoparticles with humic acid for removal of Rhodamine B in water, *J. Hazard. Mater.*, 209-210, 193–198.

[28] Zhang, X., Zhang, P., Wu, Z., Zhang, L., Zeng, G., and Zhou, C., 2013, Adsorption of methylene blue onto humic acid-coated Fe_3O_4 nanoparticles, *Colloids Surf., A*, 435, 85–90.

[29] Tombácz, E., Horvát, M., and Illés, E., 2006, Magnetite in aqueous medium: coating its surface and surface coated with it, *Rom. Rep. Phys.*, 58 (3), 281–286.

[30] Carlos, L., Cipollone, M., Soria, D.B., Moreno, M.S., Ogilby, P.R., Einschlag, F.S.G., and Martire, D.O., 2012, The Effect of Humic Acids Binding to Magnetite Nanoparticles on The Photodegradations of Reactive Oxygen Species, *Sep. Purif. Technol.*, 91, 23–29.

[31] Wu, S., Sun, A., Zhai, F., Wang, J., Xu, W., Zhang, Q., and Volinsky, A.A, 2011, Fe_3O_4 magnetic nanoparticles synthesis from tailings by ultrasonic chemical co-precipitation, *Mater. Lett.*, 65 (12), 1882–1884.

[32] Janos, P., Kormunda, M., Novak, F., Zivotsky, O., Fuitova, J., and Pilarova, E., 2013, Multifunctional humate-based magnetic sorbent: Preparation, properties and sorption of Cu(II), phosphates and selected pesticides, *React. Funct. Polym.*, 73 (1), 46–52.

[33] Koesnarpadi, S., Santosa, S.J., Siswanta, D., and Rusdiarso, B., 2015, Synthesis and characterization of magnetite nanoparticle coated humic acid (Fe_3O_4/HA), *Procedia Environ. Sci.*, 30, 103–108.

[34] Laurent, S., Forge, D. Port, M. Roch, A. Robic, C. Vander Elst, M., Muller, R.N., 2008, Magnetic iron oxide nanoparticles: Synthesis, stabilization, vectorization, physicochemical characterizations, and biological applications, *Chem. Rev.*, 108 (6), 2064–2110.

[35] Environmental Protection Agency, 1978, *Method 4.301 Phenolics*, (Spectrophotometric, manual 4AAP with distillation).

[36] Ingole, R.S., Lataye, D.H., Dhorabe, P.T., 2016, Adsorption of phenol onto banana peels activated carbon, *KSCE J. Civ. Eng.*, 21 (1), 100–110.

[37] Kyzas, G.Z. and Matis, K.A., 2015, Nanoadsorbents for pollutants removal: A review, *J. Mol. Liq.*, 203, 159–168.

[38] Ho, Y.S., and Mckay, G., 1999, Pseudo-second order model for sorption processes, *Process Biochem.*, 34 (5), 451–465.

[39] Santosa, S.J., 2014, Sorption kinetics of Cd(II) species on humic acid-based sorbent, *CLEAN Soil Air Water*, 42, 760–766.

[40] Ahmazurahman, M., 2008, Adsorption of phenolic compounds on low-cost adsorbents: A review, *Adv. Colloid Interface Sci.*, 143 (1-2), 48–67.

[41] Ahmazurahman, M., and Sharma, D.K., 2005, Adsorption of phenols from wastewater, *J. Colloid Interface Sci.*, 287 (1), 14–24.